ASSESSING THE ACCURACY OF PPP

G. Seepersad, S. Bisnath

Department of Earth and Space Science and Engineering, York University, Toronto, Ontario, M3J 1P3 Canada
gseeper@yorku.ca, sbisnath@yorku.ca

KEY WORDS: PPP, PPP accuracy, PPP convergence, GPS, GNSS, PPP limitations, PPP error budget

ABSTRACT:

The Precise Point Positioning (PPP) GNSS data processing technique has developed over the past 15 years to become a standard method for growing categories of positioning and navigation applications. The technique relies on single receiver point positioning combined with precise satellite orbit and clock information and high-fidelity error modelling. This paper uniquely addresses the current accuracy of the technique, and explains the limits of performance, which will be used to define paths for future improvements to the technology.

For geodetic purposes, performance typically refers to daily static position accuracy. PPP processing of over 300 IGS stations over one week results in few millimetre positioning rms error in the north and east components and centimetre-level in the vertical (all one sigma values). These results are categorised into quality classes in order to analyse the root causes of the resultant errors: “best”, “worst”, multipath, site displacement effects, satellite availability and geometry, etc. Also of interest in PPP performance is solution convergence period. Static, conventional solutions are slow to converge, with approximately 35 minutes required for 95% of solutions to reach the 20 cm or better horizontal accuracy.

From the above analysis, the limitations of PPP and the source of these limitations are isolated, including site displacement modelling, geometric measurement strength, pseudorange noise and multipath, etc. It is argued that new ambiguity resolution and multi-GNSS PPP processing will only partially address these limitations. Improved modelling is required for: site displacement effects, pseudorange noise and multipath, and code and phase biases. As well, more robust undifferenced-phase ambiguity validation and overall stochastic modelling is required.

1. INTRODUCTION

The Precise Point Positioning (PPP) GNSS data processing technique relies on single receiver point positioning combined with the use of precise satellite orbit and clock information and high-fidelity error modelling. Over the past 15 years PPP has become a standard method for growing categories of positioning and navigation applications. This includes, but is not limited to, crustal deformation monitoring, near real-time GNSS meteorology, orbit determination of low Earth orbiting satellites and precise positioning of mobile objects. The main commercial applications of PPP are in the agricultural industry for precision farming, marine applications for sensor positioning in support of seafloor mapping and marine construction, and airborne mapping, for photogrammetric sensor positioning (Bisnath and Gao, 2009).

PPP is currently capable of providing centimetre and decimetre-level positioning accuracy in static and kinematic mode after convergence. The results presented in Bisnath and Gao (2009) indicates that it takes approximately 20 to 30 minutes for the positioning solution to converge to the centimetre-level in static mode. The final positioning accuracy of float PPP in static mode presented by Ge et al, (2008) was 3, 4 and 8 mm in north, east and up components respectively. With the implementation of ambiguity resolution (PPP-AR) the rms for the east component was reduced from 4 to 3 mm and even smaller improvements were observed in the north and up components. This paper uniquely addresses the current accuracy of float PPP, explains the limits of performance, and defines paths to improvements.

2. FUNDAMENTAL CONCEPTS OF PPP

In single point positioning, the coordinates of a receiver at an "unknown" point are sought with respect to a geodetic datum by using the "known" positions of the GNSS satellites being tracked. Single point positioning (also referred to as absolute positioning or point positioning) is the most basic GNSS solution obtained with epoch-by-epoch least-squares estimation. For point positioning, GPS provides two levels of services, the Standard Positioning Service (SPS) with access for civilian users and the Precise Positioning Service (PPS) with access for authorized users. In SPS, only the C/A-code is available. The achievable real-time SPS 3D positioning accuracy is ~10 m at the 95% confidence level (Hofmann-Wellenhof et al, 2001).

Similar to single point positioning, PPP allows for the estimation of a state space solution using undifferenced GNSS observations collected using a single GNSS receiver. The development of PPP became a possibility with the development of time interpolated precise orbits and clocks, which, unlike broadcast orbits with an accuracy of approximately 1 m for satellite orbits and 5 ns for satellite clocks, the highest quality precise satellite orbits and clocks have an accuracy of 2.5 cm and 75 ps, respectively (IGS, 2013). PPP also takes full advantage of the precise but ambiguous carrier-phase observations and relatively noisy pseudoranges.

It is necessary when processing data with PPP to mitigate all potential effective error sources in the system. As a result of the un-differenced nature of PPP, all errors caused by the space segment, signal propagation and signal reception at the antenna then receiver directly impact the positioning solution. Error mitigation can be carried out by modelling, estimating or eliminating (through linear combination) each error term. These basic fundamental differences between SPS and PPP are highlighted in Figure 1.

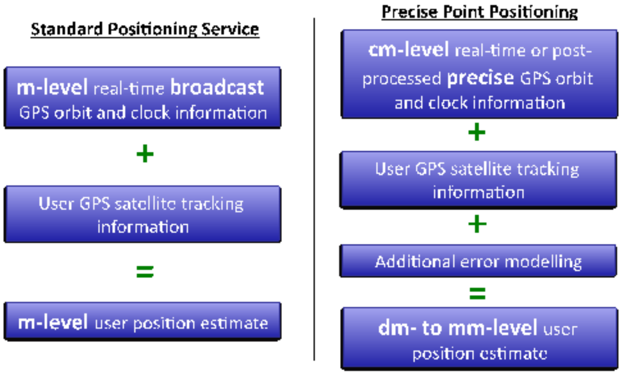

Figure 1. Overview of SPS and PPP

2.1 Defining PPP error budget

Each GNSS has been designed to perform with a high level of precision. However, there still remain numerous errors sources to be accounted for on the pseudorange or carrier-phase observations to eliminate effects such as special and general relativity, Sagnac delay, satellite clock offsets, atmospheric delats, etc. These errors can cause a combined deviation of +/- 50-100 m and must be considered even for single point positioning.

When attempting to combine satellite positions and clocks precise to a few centimetres with ionospheric-free pseudorange and carrier phase observations, it is important to account for some effects that may not have been considered in SPS. Also, defining this error budget becomes more challenging as these error sources can be subdivided into errors projected onto the range and localized site displacements. This situation is illustrated in Figure 2. As the signal is transmitted from the satellite to the receiver, error sources affected in the range domain include satellite and receiver clock error, atmospheric and relativistic, multipath and noise and carrier phase wind-up. Site displacement effects occur at the satellite and receiver and these include effects such as phase centre offset and variation, orbit and clock errors, and at the receiver, solid Earth tides and ocean loading.

Aside from this range to position domain transformation, PPP using sequential filtering (typical Kalman or least-squares) in the form of position domain Hatch filtering to reduce the effects of pseudorange noise and multipath and increase the weight of the change in carrier-phase measurements.

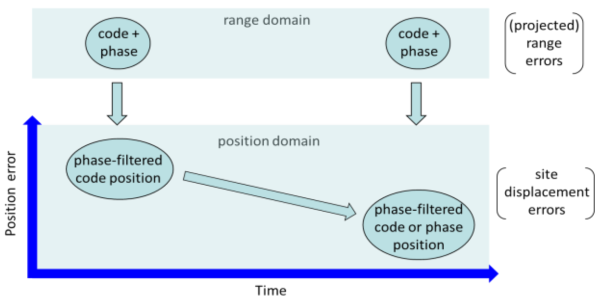

Figure 2: Range to position domain and time domain transformations in PPP data processing

2.2 PPP Error management

As previously mentioned, there are a few corrections which have to be applied to pseudorange and carrier-phase measurements, in addition to other commonly known effects such as relativistic correction in order to have a complete observation model in PPP. The observation model of PPP is assumed known, and hence will not be discussed. Interested readers can review, e.g., Zumberge et al. (1997) and Kouba and Héroux (2001). Presented in Table 1 is a summary of all corrections accounted for and the applied mitigative strategy.

A dual-frequency GNSS receiver is typically used to mitigate the first-order effect of ionospheric refraction. A linear combination of the dual-frequency pseudorange and carrier phase measurements will reduce the effects on the range from 10's of metres to few millimetres. For the tropospheric refraction, which has an effect of a few metres on the range, the dry component is modelled and the wet component is estimated along with user positioning and ambiguity terms, resulting in a few millimetre residual error. To achieve the highest PPP positioning accuracy, error sources such as tidal loading, phase wind-up and antenna phase offset and variation at the satellite and receiver are modelled. Residual terms such as pseudorange and carrier phase multipath and noise are typically filtered, stochastically de-weighted or simply ignored.

Effect	Magnitude	Domain	Mitigation method	Residual error
Ionosphere	10s m	range	linear combination	mm
Troposphere	few m	range	modelling; estimation	dm - mm
Relativistic	10 m	range	modelling	mm
Sat phase centre; variation	m - cm	pos; range	modelling	mm
Code multipath; noise	1 m	range	filtering	dm - mm
Solid Earth tide	20 cm	position	modelling	mm
Phase wind-up (iono-free)	10 cm	range	modelling	mm
Ocean loading	5 cm	position	modelling	mm
Satellite orbits; clocks	few cm	pos; range	filtering	cm - mm
Phase multipath; noise	1 cm	range	filtering	cm - mm
Rcv phase centre; variation	cm - mm	pos; range	modelling	mm

Table 1. Summary of error sources in PPP and mitigative strategy

2.3 Limitations of PPP

While PPP presents definite advantages, there are still underlying limitations, which are the focus of most current PPP research activities.

2.3.1 *Convergence*

PPP requires a relatively long initialization period (few tens of minutes at least) for the carrier-phase ambiguities to converge to constant values and for the solution to reach its optimal precision. This situation is primarily caused by the estimation of the carrier-phase ambiguities from the relatively noisy pseudoranges. This allows PPP to take full advantage of the precise but ambiguous carrier-phase observations; however, the length of time it takes to reach the optimal solution is a major disadvantage to the wider use of the technique. If the pseudoranges were more precise there would be a reduction in the convergence period (Bisnath and Gao, 2009; Seepersad, 2012). PPP-AR would accelerate the overall solution convergence to give cm-level horizontal accuracy after 1 hour or less. The results presented by Collins et al, (2010) show after 1 hour 90% of the solutions approach 2 cm horizontal error, compared to 10 cm for the float PPP solution.

2.3.2 *Pseudorange multipath and noise*

Pseudorange multipath and noise together are the largest remaining unmanaged error source in PPP. By reducing the effects of the multipath and noise on the pseudorange observables, the carrier-phase ambiguities will reach a steady state at an earlier time, thus reducing the initial and re-convergence period of PPP as well as decreasing the time required for PPP-AR to resolve ambiguities (Seepersad and Bisnath, 2012).

2.3.3 *Integrity Monitoring*

Integrity monitoring is an essential component of any positioning / navigation system. PPP integrity indicators include post-fit residuals, processing filter convergence, and parameter estimation covariance. Given that in PPP processing some parameters are estimated while others are eliminated, without multiple solutions (as in the case with double-differenced static, multi-baseline networks and network RTK) providing integrity information for PPP single receiver estimates is all that more important. Post-fit residuals from PPP epoch solutions could be analysed to detect individual measurement outliers, or more significant problems. Also, the covariance of the estimated position can be used as an indicator of the solution accuracy in PPP, as a reference solution may not always be available (Bisnath and Gao, 2009; Seepersad, 2010).

2.3.4 *Quality of models*

In PPP, undifferenced GNSS observations are collected using a single GNSS receiver. This requires error sources such as tidal loading, carrier phase wind-up, antenna phase offset and clock errors to be accurately accounted for, as opposed to (short baseline static) relative positioning, as these errors are eliminated through measurement differencing. There is a requirement for these models to perform at the utmost integrity to assure the highest accuracy is provided to the user. This is a challenging task, as error sources such as solid and ocean tidal loading are localized to the receiver.

2.3.5 Real-time PPP

PPP requires only one GNSS receiver; no differencing between receivers and satellites can be computed to eliminate satellite specific errors such as clock and orbital errors. Therefore, it is necessary to use the most precise satellite clock corrections and satellite orbits. An IGS real-time service has been publically available as of April 2013 allowing the possibility of real-time PPP orbits and clocks with a precision of 5 cm and 1.5 ns respectively. The performance of PPP is limited by the quality of these products as Final IGS orbits and clocks with an accuracy of 2.5 cm and ~75 ps, respectively (IGS, 2013).

2.3.6 *Single-frequency*

With single-frequency PPP, the ionospheric-free linear combination cannot be created. This requires two alternatives, either a linear combination of the L1 pseudorange and carrier phase signals or obtain external information about the ionospheric delay. The major limitation of the first technique is the required estimation of the carrier-phase ambiguity. Therefore, the initial position estimates would further deteriorate and a longer convergence time is required. Ionospheric delay estimates can be obtained from agencies such as the IGS. Currently, IGS final ionospheric TEC grid has a precision of 2-9 TECU at a time interval of two hours. This uncertainty maps into range errors in the order of 30 cm up to 1 m, respectively (IGS, 2013). Single-frequency GNSS PPP has been investigated with great promise for certain applications (see, e.g., Gao et al. (2006) and Choy et al. (2009)).

3. EXAMINING CURRENT ACCURACY AND LIMITATIONS OF PPP

This section quantifies the current accuracy and convergence of PPP in static and kinematic processing modes for a very large set of globally distributed sites. This is followed by analysis of the global distribution of horizontal and vertical position biases of all processed sites. Also, a unique analysis of how PPP position biases and convergence vary within a small graphic region and possible causes is provided.

3.1 Dataset and processing parameters

GPS data from 300 IGS stations observed during DOY 183 to 189 in 2012 were processed using the York-PPP software. York-PPP was developed based on the processing engine used by the on-line CSRS-PPP service (NRCan, 2010). The sites chosen were a subset of those processed regularly by most IGS ACs, representing a good global distribution. The distribution of the sites is illustrated in Figure 3. Dual-frequency receivers tracking either the C/A or P(Y) pseudorange on L1 were used. Settings used for the evaluation include the ionosphere-free combination of L1 and L2 data, 2 m and 15 mm a priori standard deviations for pseudorange and carrier-phase observations, respectively, and a 10° elevation cut-off angle.

IGS final 5 minute orbits and 30 second clocks and products were used. The reference stations were analysed in static and kinematic PPP mode. Receiver clocks were estimated epoch-by-epoch. The zenith tropospheric delays were estimated every 60 minutes with an initial standard deviation of 1 m and a power density of 2 cm/sqrt (h). The station coordinates were estimated with an initial constraint of 1 km. The IGS relative antenna model file was used and ocean loading and solid Earth tides were obtained from Scherneck (2011) for each of the sites being processed.

Figure 3. Global distribution of the selected 300 IGS stations

3.2 Conventional Static PPP Results

To quantify the accuracy of PPP, the estimated positions were compared with the IGS weekly SINEX solution (Crustal Dynamics Data Information System, 2012). The primary factors that affect the convergence period and the accuracy of PPP are the limited precision of current precise orbit and clock products and the effects of unmodelled error sources. Solution here refers to the solution generated after processing the entire 24 hour dataset. The distribution of the solutions in the horizontal and vertical components is illustrated in Figure 4 and Figure 5, respectively, with histogram bin sizes of 1 mm and 5 mm, respectively, for a sample size of 2010.

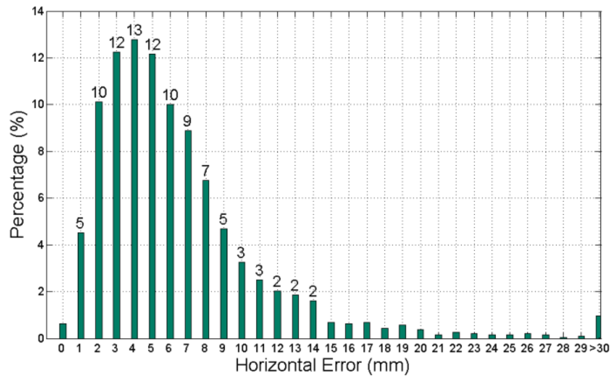

Figure 4. Histogram showing absolute horizontal error

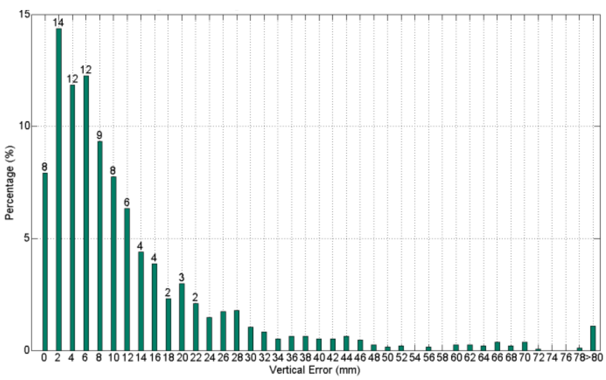

Figure 5. Histogram showing absolute vertical error

PPP is capable of producing sub-centimetre accuracy in the horizontal component and centimetre in the vertical. 99% of the data processed had an error in the horizontal component of less than or equal to 25 mm and 87% of the results had a horizontal error of less than one centimetre. In the vertical component, 99% of the data processed had an error of less than 80 mm and 95% of the results had an error less than 50 mm. It is expected for the vertical component to be of a lesser accuracy than that of the horizontal component due to satellite geometry (inherent to all modes of GNSS data processing) and the quality of the models used for atmospheric modelling and the solid Earth tides and ocean loading. A summary of the statistics of positions estimated are presented in Table 2. The solution had an rms of 5, 6 and 13 mm in the north, east and up, respectively.

The horizontal component of the software was comparable to the results presented by Ge et al., (2008) with an rms 3 and 4 mm in north and east. In the up component, the rms was 1.7 times greater than published results by Ge et al., (2008). Ge et al., (2008) carried out a 7-parameter Helmert transformation when comparing their results against the SINEX coordinates. This questionable coordinate adjustment would most likely have further reduced the biases from their results, and may explain why the accuracy of their up component is not typical of PPP. The 7-parameter Helmert transformation between the two products allows the evaluation and removal of systematic differences caused by reference frame realizations that are slightly different (Mireault et al, 2008). This transformation is not required to be carried out as the solutions produced would have been in the same coordinate system as the IGS weekly satellite orbit and coordinate products.

Absolute point positioning is calculated relative to a well-defined global reference system, in contrast to relative positioning, where the coordinates are in relation to some other fixed point. Eckl et al. (2001) describes the accuracy of static relative positioning with a geodetic-grade receiver is typically 5 mm + 0.5 ppm (rms) for the horizontal component and 5 mm + 1 ppm (rms) for the vertical component. This is the highest accuracy possible for static relative positioning, as the fixed point would have an uncertainty associated with it. To determine if it is possible to replace static relative positioning by PPP, the inverse between PPP coordinates to determine static relative error statistics were calculated from the solution estimated by York-PPP and compared to the specifications published by Eckl et al. (2001). In the horizontal component the PPP solution had an accuracy of 7 mm, which is comparable to static relative positioning. In the vertical component, the accuracy of relative positioning is 2.6 times greater than that of the PPP solution.

	max	**mean**	**std dev**	**rms**
Northing	27	-1	5	5
Easting	26	-1	6	6
Horizontal	28	1	7	7
Vertical	51	-1	13	13
3D	52	2	15	15

Table 2. Final solution produced by York-PPP from 24 hour datasets from 300 sites for DOY 183-189, processed in static mode for a total sample size of 2010. All units are in millimetres

3.3 Conventional Kinematic PPP Results

The difference between static and kinematic mode in PPP primarily exists in the variation of the process noise models in the sequential least-squares (in this case) or Kalman filter. The process noise for the coordinates serves as a priori weighted constraints to the parameters. The quantity of process noise can be scaled based on the user dynamics such as stationary, walking, driving and satellite motion with process noise values of 0 ms^{-1}, 1 ms^{-1}, 10 ms^{-1} and 10000 ms^{-1}, respectively. A process noise equivalent of that of a terrestrial vehicle in motion was used, even though overly pessimistic, it serves to better analyse the contrast in the quality of the results from static and kinematic mode and the variation of convergence.

To examine the kinematic mode of the software, the same static dataset was used to simulate kinematic data. This method of analysis was chosen due to the limited availability of reference solutions for kinematic results with a higher precision than PPP. Presented in Figure 6 and Figure 7 are the horizontal and vertical kinematic results, respectively. In the horizontal component, 98% of the data processed had an error of less than 150 mm and 95% had an error of less than 80 mm. In the vertical component, 99% of the data processed had an error less than 400 mm and 95% had an error of less than 160 mm.

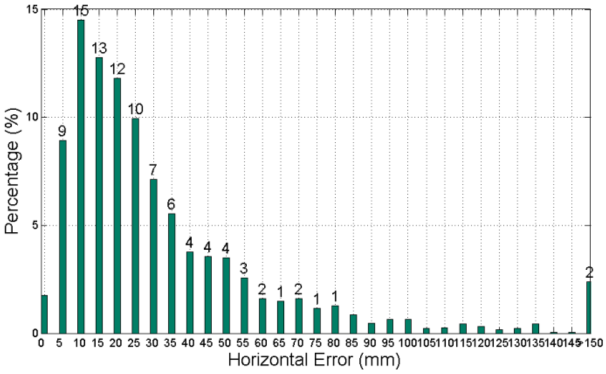

Figure 6. Histogram showing absolute horizontal error

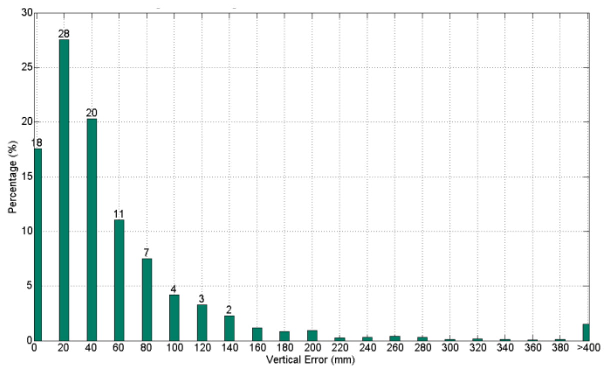

Figure 7. Histogram showing absolute vertical error

A summary of the statistics of positions estimated is presented in Table 3**.** In static mode, the horizontal component rms was 7 mm in contrast to kinematic mode which was 46 mm, and in the vertical component 13 mm in static mode and 72 mm in kinematic mode. The solution quality deteriorated because of the magnitude of the process noise used, adding large uncertainties to each parameter, allowing the solution to converge freely based on individual measurements, whereas in static mode the parameters are tightly constrained, thus a significantly higher accuracy of results is achieved through the power of averaging.

	max	mean	std dev	rms
Northing	285	3	27	27
Easting	365	-2	37	37
Horizontal	463	4	46	46
Vertical	592	-4	72	72
3D	752	63	85	85

Table 3. Final solution produced by York-PPP from 24 hour datasets from 300 sites for DOY 183-189, processed in kinematic mode for a total sample size of 2010. All units are in millimetres.

3.4 Convergence period in static and kinematic mode

PPP definitely presents advantages for many applications in terms of operational flexibility and cost-effectiveness. One of its major limitations is its relatively long initialization time as carrier-phase ambiguities converge to constant values and the solution reaches its optimal precision. PPP convergence depends on a number of factors such as the number and geometry of visible satellites, user environment and dynamics, observation quality and sampling rate (Bisnath and Gao, 2009). As these different factors interplay, the period of time required for the solution to reach a pre-defined precision level will vary.

The variation in convergence period is easily visible between static and kinematic modes as a result of the difference in the process noise applied. In static mode, the estimated parameters are constrained, allowing the ambiguities to be estimated within a shorter time period. In static mode, an exponential trend was observed in contrast to the quasi-linear trend in kinematic mode. In static mode, 25% of the solutions had an initial horizontal error of 20 cm or less, and 20% in kinematic mode. Within 10 minutes 85% of data processed had met the horizontal accuracy threshold, but an additional 15 minutes was required for 96% of the data to converge. It took approximately 25 minutes for 75% of the solutions to converge in kinematic mode and 55 minutes for 89% of the solutions. For various applications of PPP, it would be recommended to collect an initial 15 minutes of data while the receiver is stationary, after which the receiver can be moved to collect data at various locations. The initial 15 minutes can be processed in static mode allowing solution to converge within a shorter time period, after which the convergence mode can be switched to kinematic and the receiver moved.

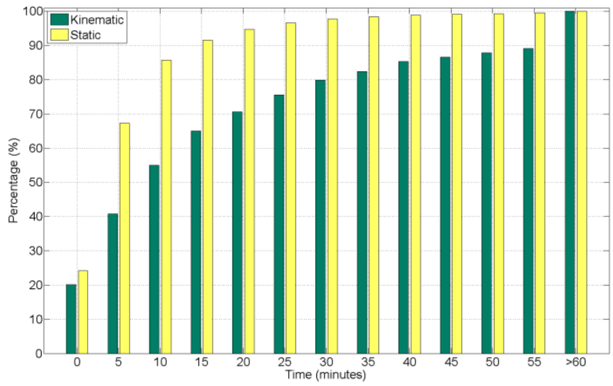

Figure 8. Cumulative histogram showing convergence period to 20 cm horizontal accuracy for static and kinematic PPP

3.5 Distribution of position biases

Position repeatability can quantitatively reflect the intrinsic positioning quality of PPP. The position repeatability was generated by computing the station-specific positions over one week and then computing the average of the resulting residuals for each site. Overall, in the horizontal component all stations had a bias of 1 mm in the horizontal and -1 mm in the vertical when processed in static mode. Illustrated in Figure 9 and Figure 10 is the geographical distribution of the station-specific position differences in the horizontal and vertical components, respectively. In the horizontal component, no visible trends are noticed when the weekly average for each site is examined. In the vertical component, the absolute bias is examined. In the horizontal, 87% of the data had an error of less than one centimetre in contrast to vertical component, where only 67% of the data had an error less than one centimetre. The vertical biases greater than 3 cm, were mostly located around coastal regions.

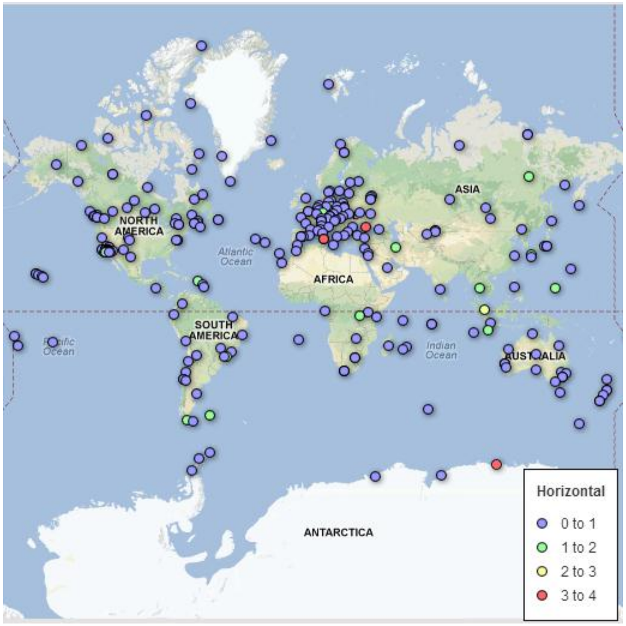

Figure 9. Geographical distribution of the station-specific position differences in the horizontal component processed in static mode for GPS week 1695

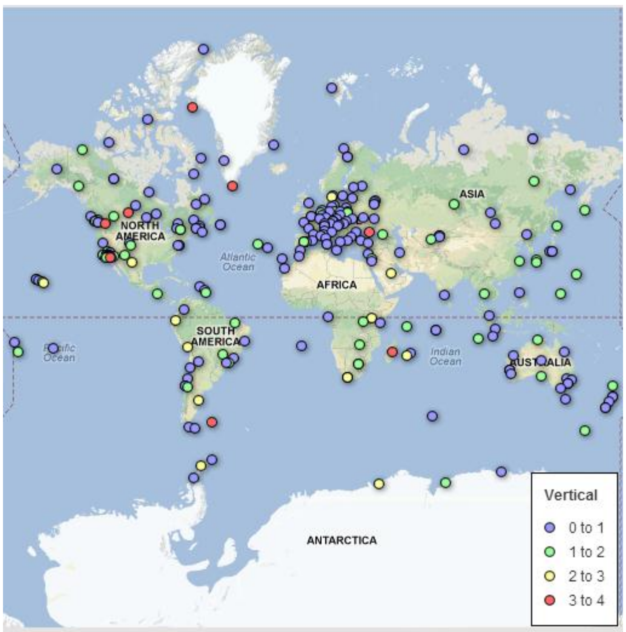

Figure 10. Geographical distribution of the station-specific position differences in the vertical component processed in static mode for GPS week 1695

To further highlight the variations of PPP solution, Figure 11 contains 5% of the "best" and "worst" horizontal solutions. The figure dramatically shows how accurate the "best" solutions are, with virtually no bias or variance, while the "worse" solutions contain centimetre level dispersion. Further analysis is required to determine if there is a root cause or causes of these solution variations, or if the variations reflect the limits of the processing technique. Figure 12 illustrates the geographical distribution "best" and "worst" 5% of horizontal solutions highlighted in blue and red respectively. The "worst" datasets are most noticeable in regions where the IGS has a weaker densification of continuously operating reference stations and around the city of Los Angeles, which is affected by the Pacific Plate, as its moving northwards with respect to the North American Plate.

To further quantify the distinction between the "best" and "worst" horizontal solutions, the sites were further examined with respect to the number of satellites, position dilution of precision (PDOP), monument receiver, antenna and clock type. No noticeable trends were observed.

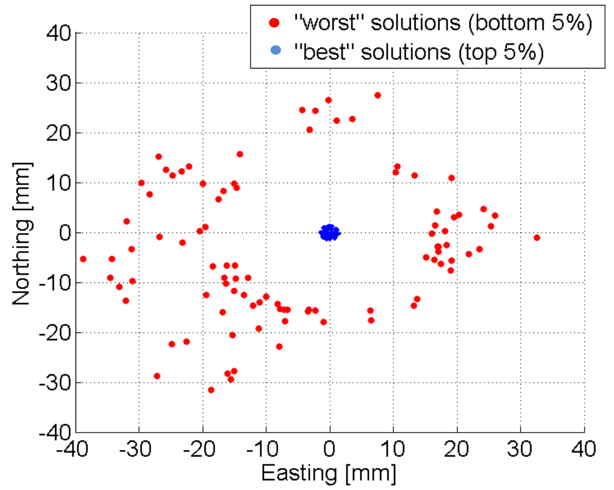

Figure 11. "Best" and "worst" 5% of PPP horizontal solutions as compared to weekly IGS SINEX solution

Figure 12. Geographical distribution of the "Best" and "worst" 5% of PPP horizontal solutions as compared to weekly IGS SINEX solution highlighted in blue and red, respectively.

Of the 2010 datasets, the "best", "average" and "worst" datasets were selected based on the quality of the horizontal position for further analysis. The convergence for northing, easting and up components for each dataset is presented in Figure 13, Figure 14 and Figure 15. Table 4 is a summary of the statistics for each of the three sites with respect to their weekly solutions. The site RIGA, located in Latvia, Northern Europe had the best convergence of all datasets processed on DOY 186 with a horizontal and vertical difference of 0 and 1 mm, respectively. The weekly solution had an average difference of 3 mm and standard deviation of 2 mm in the horizontal and an average difference of 3 mm and standard deviation of 5 mm in the vertical. The solution achieves a steady state of 20 cm horizontal within the first 5 minutes.

Site		Horizontal	Vertical
RIGA	Weekly	3 +/- 2	3 +/- 5
	DOY: 186	0	1
CONT	Weekly	9 +/- 2	-11 +/- 2
	DOY: 189	5	-6
POVE	Weekly	29 +/- 10	-1 +/- 10
	DOY: 189	39	-12

Table 4. Summary of the position difference of the "best", "average" and "worst" datasets. All units are in millimetres.

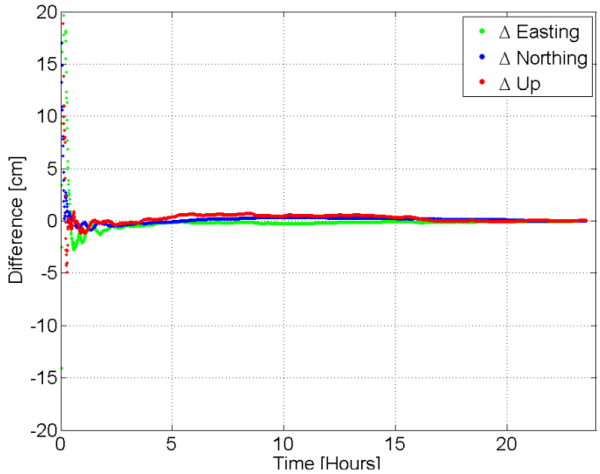

Figure 13. Site RIGA DOY 186 showing "best" convergence solution in static mode

The site CONT, located in Concepcion, Chile showed average convergence of all datasets processed on DOY 189 with a horizontal and vertical difference of 5 and -6 mm, respectively. The weekly solution had an average difference of 9 mm and standard deviation of 2 mm in the horizontal and an average difference of -11 mm and standard deviation of 2 mm in the vertical. The solution achieves a steady state of 20 cm horizontal within the first 15 minutes.

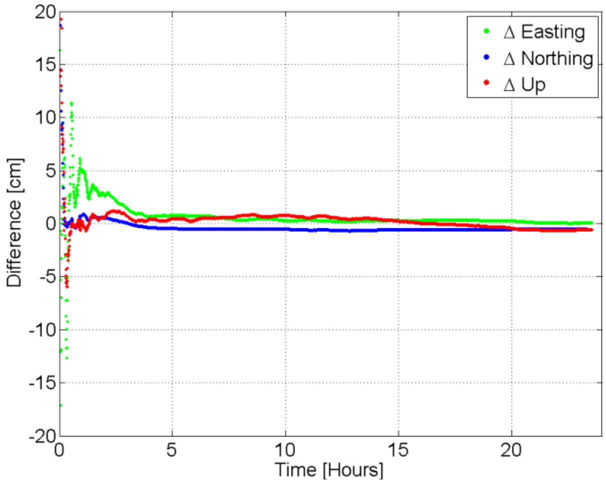

Figure 14. Site CONT DOY 189 showing "average" convergence solution in static mode

The site POVE on DOY 189, had the worst horizontal solution of all the datasets processed. The site is located in Porto Velho, Brazil. The dataset had a horizontal and vertical difference of 39 and 12 mm, respectively. The weekly solution had an average difference of 29 mm and standard deviation of 10 mm in the horizontal and an average difference of -1 mm and standard deviation of 10 mm in the vertical. The solution achieves a steady state of 20 cm horizontal within the first 20 minutes. A few centimetre divergence is noted only in the east component with sub-centimetre accuracy in the north component and centimetre-level in the up component. This may be due to undetected cycle slips.

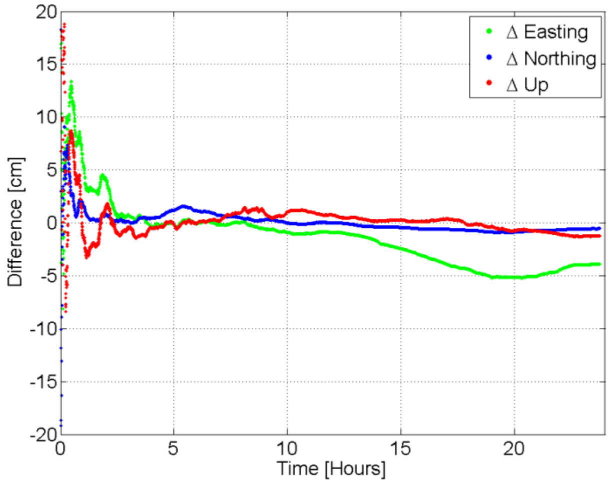

Figure 15. Site POVE DOY 189 showing "worst" convergence solution in static mode

3.6 Analysis of varying convergence and position biases

As previously discussed, PPP convergence is affected by several different factors. To better understand the factors affecting convergence, 8 active control points were selected within the city of Los Angeles. This area was selected because of the dense network and varying position quality amongst the stations. Summarized in Table 5 is the monument description and receiver, antenna and clock type for each of the stations.

Site	Receiver	Antenna	Clock	Monument Description
AZU1	TRIMBLE NETRS	ASH701945B_M	Internal	shallow rod
LEEP	TPS NET-G3A	TPSCR.G3	Internal	shallow rod
CLAR	TPS NET-G3A	TPSCR.G3	Internal	shallow rod
CHIL	TPS NET-G3A	TPSCR.G3	Internal	rock-pin/metal-tripod
JPLM	ROGUE SNR-8100	AOAD/M_T	Rubidium	brass plate
JPLV	JPS EGGDT	JPLD/M_R	N/A	brass plate
CIT1	ASHTECH Z-XII3	TPSCR.G3	Internal	wall
WHC1	TPS NET-G3A	TPSCR.G3	Internal	pillar

Table 5. Summary of site information (SOPAC, 2013)

Illustrated in Figure 16 and Figure 17 are the distribution of the weekly averaged biases for the horizontal and vertical components. In the horizontal component, sub-centimetre variation amongst all the sites had an error of less than 1 cm. In the vertical component centimetre variation is observed. In the vertical component, sites such as JPLM, JPLV, AZU1 and WHC1 performed above average as biases were less than one centimetre.

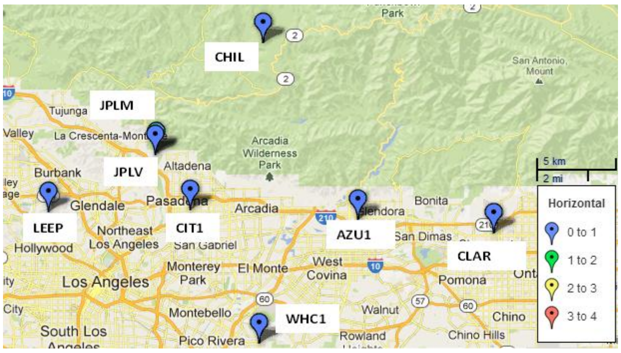

Figure 16. Geographic distribution of the average horizontal position difference

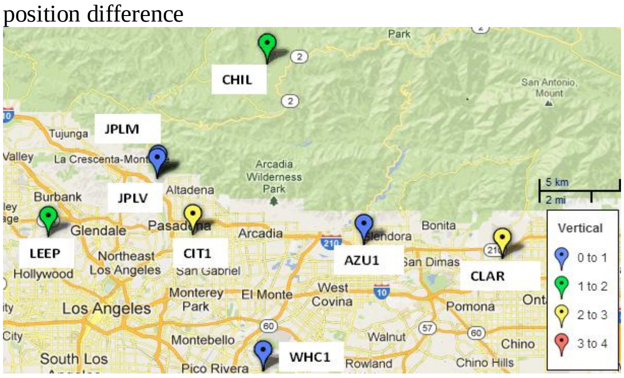

Figure 17. Geographic distribution of the average vertical position difference

The PDOP and number of satellites for the sites CIT1 and JPLM are illustrated in Figure 18 and Figure 19 respectively. CIT1 and JPLM were selected as they were within 5 km of each other and the average position difference of CIT1 was 2 cm greater than that of JPLM. The PDOP of JPLM was greater than that of CIT1 with a standard deviation of 1.3 and 1, respectively. The spikes in the PDOP at the site JPLM was due to relatively low number of satellites with a minimum of 5 and maximum of 8 in contrast to CIT1, which had a minimum of 8 and maximum of 12. CIT1 is located on the California Institute of Technology which has clear sky coverage in contrast to JPLM, which has a lesser number of satellites as it is located south-west of a national forested area with an altitude ranging from 372 m (altitude of JPLM) to 1567 m (altitude of CHIL). While the site CIT1 had a lower PDOP and more satellites indicating a strong satellite geometry, the quality of data from the site JPLM provided a better solution quality indicating that more satellites and a strong geometry may not always provide a higher quality solution.

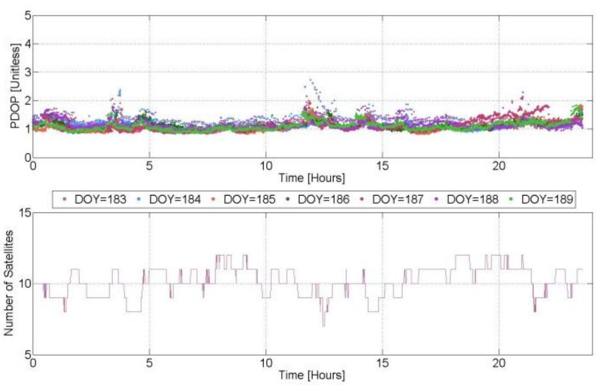

Figure 18. The PDOP (upper plot) and the number of satellites (lower plot) for DOY 183-189 of 2012 for the site CIT1

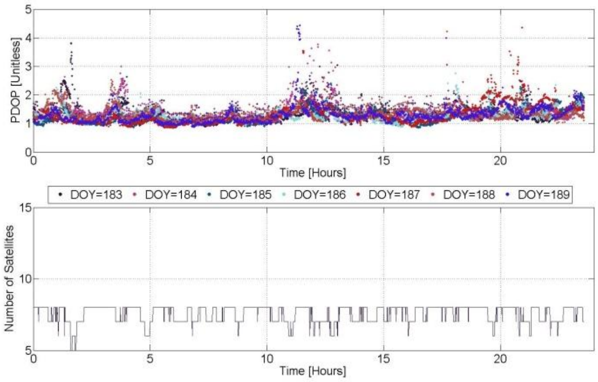

Figure 19. The PDOP (upper plot) and the number of satellites (lower plot) for DOY 183-189 of 2012 for the site JPLM

The term convergence in this analysis refers only to the initial 2 hours of PPP processing, as the final solution of all sites the met the expected accuracy of PPP. The weekly convergence trends of all 8 sites were examined; AZU1 and CLAR had the worst convergence and LEEP had below average quality of convergence. All the other sites showed good convergence where a steady state was attained within the first 30 minutes of processing. Presented in Figure 20 and Figure 21 is the horizontal convergence for the sites AZU1 and WHC1 illustrating the worst and best convergence, respectively.

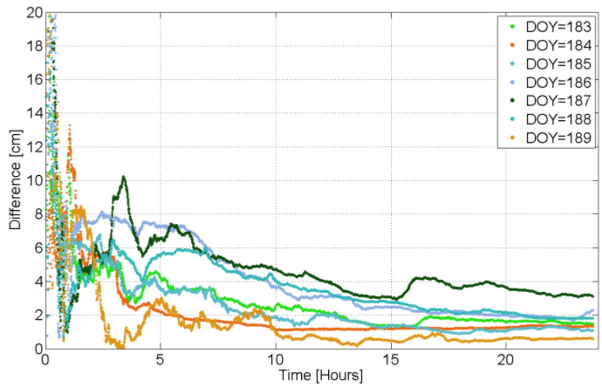

Figure 20. Site AZU1 DOY 183-189 showing poor horizontal convergence in static mode

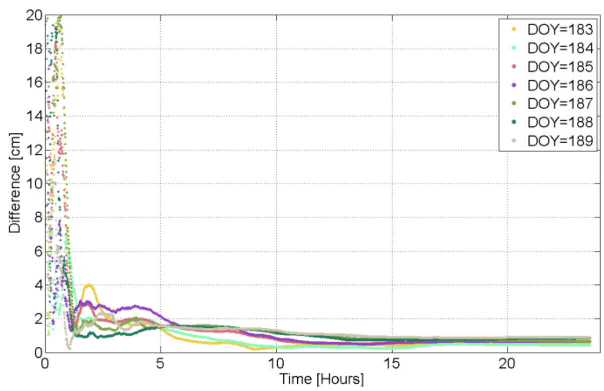

Figure 21.Site WHC1 DOY 183-189 showing typical convergence in static mode

The most consistent trend were at the sites AZU1, CLAR and LEEP where monuments were "shallow rods". This may cause increase effects of multipath as the receivers may be susceptible to multipath from under the receiver. Also, typical of lower cost monuments are situated in areas such as urban canyons where insufficient room is available to construct permanent and stable monuments such as pillars.

To quantify the magnitude of multipath present at each site, the so-called pseudorange multipath observable is computed (see, e.g., Hofmann-Wellenhof et al. (2001). This estimate represents a linear combination of the measured pseudorange and carrier-phase measurements. The multipath observable consists primarily of the pseudorange multipath and variations from instrumental delays. Illustrated in Figure 22 is an overlay of the multipath observable for PRN 06 for the sites AZU1, WHC1 and CLAR. For PRN 06, at the site AZU1 had the largest standard deviation of 62 cm followed by WHC1, LEEP and CLAR with standard deviations of 58, 57 and 47 cm respectively. This trend was observed for all satellites indicating multipath may not be the primary factor for poor initial convergence at AZU1 and CLAR.

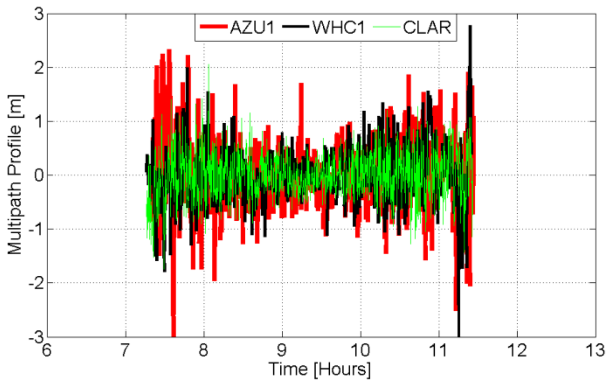

Figure 22. Comparing the pseudorange multipath profile for PRN 06 at AZU1, WHC1 and CLAR, for DOY 183 of 2012

The standard deviation of the pseudorange residuals of the sites AZU1, CLAR and LEEP were calculated at a 30° bin and compared to WHC1. The trend present at WHC1 was as expected, where the standard deviation was indirectly proportional to the standard deviation. At elevation angle 10° - 30° the residuals had a standard deviation of 1.12 m in contrast to 60° - 90° with a standard deviation of 0.90 m. At the three sites AZU1, CLAR and LEEP the residuals showed similar trends where the standard deviation increased with the elevation angle. The most significant change was observed at CLAR where at 10° - 30° whose standard deviation was the smallest of the four sites with a value of 1.03 m and at 60° - 90° the standard deviation was the largest with a value of 0.90 m.

Site	Standard Deviation (m)		
	0° - 30°	30°- 60°	60° - 90°
AZU1	1.3	1.15	1.18
WHC1	1.12	1.08	0.90
CLAR	1.03	1.29	1.49
LEEP	1.11	1.27	1.42

Table 6. Standard deviation of the pseudorange residuals with a 30° bin size, for all satellites, on DOY 183 of 2012

Presented in Figure 23 is an overlay of the pseudorange residuals of all satellites for the sites AZU1 and WHC1. 95% of the residuals of WHC1 ranged between ± 2.13 m with a standard deviation of 0.670 m while at AZU1 95% of the residuals were between ± 2.42 m with a standard deviation of 0.76 m.

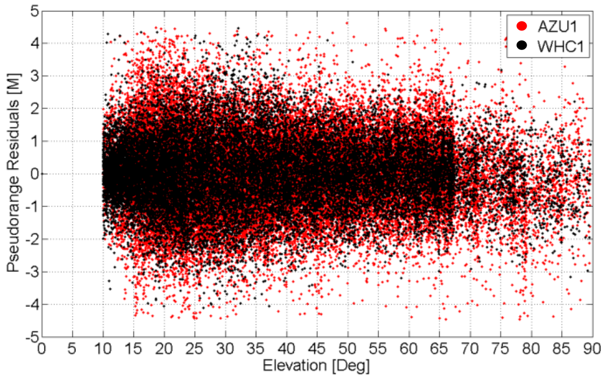

Figure 23. Comparing the pseudorange residuals for the sites AZU1 (red) and WHC1 (black) for all satellites, for DOY 183 of 2012

4. CONCLUSIONS AND FUTURE WORK

Current limitations of PPP such as the relatively long initial convergence time, quality of the current PPP models, pseudorange multipath and noise mitigation, real-time PPP and single frequency PPP are addressed. Also presented is the PPP error budget and some of the challenges in defining the error budget as the error sources can be subdivide into errors projected onto the range and localized site displacements.

The current accuracy of PPP was assessed by processing GPS data from 300 IGS stations observed during DOY 183 to 189 in 2012. IGS accumulated weekly SINEX station coordinates was used as the reference solution. In static mode, the accuracy was 7 and 13 mm in the horizontal and vertical components respectively. In kinematic mode, the accuracy of the horizontal component was 46 mm and 72 mm in the vertical component. The solution quality deteriorated because of the magnitude of the process noise used, adding large uncertainties to each parameter, allowing the solution to converge freely based on individual measurements, whereas in static mode the parameters are tightly constrained, thus a significantly higher accuracy of results is achieved through the power of averaging. Static, conventional solutions are slow to converge, with approximately 35 minutes required for 95% of solutions to reach the 20 cm or better horizontal accuracy. In kinematic mode, it took 55 minutes for 89% of data. For various applications of PPP, it would be recommended to collect an initial 15 minutes of data while the receiver is stationary, after which the receiver can be moved to collect data at various locations.

Factors that possibly affect quality of convergence are examined within a test site located in Los Angeles consisting of 8 active control points. Some of the factors examined include monument type and receiver, antenna and clock type for each of the stations. Also analysed was the geometric measurement strength, pseudorange multipath and noise and pseudorange residuals. It's also noted, the sensitivity of the receiver and its effects on the quality of the PPP convergence and final solution.

Further analysis is required to determine if there is a root cause or causes of these solution variations, or if the variations reflect the limits of the processing technique. Additional work would also include upgrading the York-PPP software to process GLONASS and Galileo data, as well as work on the functionality of the software to allow for a real-time solution as real-time IGS data streams are now publically available.

5. ACKNOWLEDGEMENTS

The research reported in this paper was funding from the Natural Sciences and Engineering Research Council of Canada. The results presented in this paper are derived from data and products provided by Natural Resources Canada and the International GNSS Service.

6. REFERENCES

Bisnath, S. and Y. Gao (2009) Current state of precise point positioning and future prospects and limitations, *International Association of Geodesy Symposia*, Vol. 133, pp. 615-623.

Choy SL (2009) An investigation into the accuracy of single frequency PPP, [*Ph.D. Thesis*], RMIT University, Melbourne, Australia.

Collins, P., S. Bisnath, F. Lahaye, and P. Héroux (2010) Undifferenced GPS Ambiguity Resolution Using the Decoupled Clock Model and Ambiguity Datum Fixing, *ION GNSS*, Vol. 57, No. 2, pp. 123-135.

Crustal Dynamics Data Information System (2012) ftp://cddis.gsfc. nasa.gov/pub/gps/ products/1651.

Eckl, M.C., R. Snay, T. Soler, M.W. Cline, and G.L. Mader (2001) Accuracy of GPS derived relative positions as a function of interstation distance and observing session duration, *Journal of Geodesy*, Vol. 75, pp. 633-640.

Gao, Y., Y. Zhang and K. Chen (2006). "Development of a real-time single-frequency Precise Point Positioning system and test results." Proceedings of ION GNSS 2006, Fort Worth, Texas, pp. 2297-2303.

Ge, M., G. Gendt, M. Rothacher, C. Shi, and J. Liu (2008) Resolution of GPS carrier-phase ambiguities in precise point positioning (PPP) with daily observations, *Journal of Geodesy*, Vol. 82, No. 7. pp 65-78

Hofmann-Wellenhof, B., H. Lichtenegger, and J. Collins (2001) *GPS Theory and Practice*, New York: Springer Wien.

IGS (2013) IGS Products, http://igscb.jpl.nasa.gov/components/prods.html, accessed April 2013.

Kouba, J. and Pierre Héroux (2001) Precise Point Positioning Using IGS Orbit and Clock Products, *GPS Solutions*, Vol. 5, No. 2, pp. 12-28.

Mireault Y., P. Tétreault, F. Lahaye, P. Héroux, and J. Kouba, 2008, "Online Precise Point Positioning: A New, Timely Service from Natural Resources Canada," *GPS World*, Vol. 19, no. 9, pp. 59 – 64.

NRCan (2010) About Us, http://www.nrcan-rncan.gc.ca/com/index-eng.php, accessed April 2013

Scherneck, H.-G. (2011) Ocean Tide Loading Provider, http://froste.oso.chalmers.se/ loading//index.html, accessed April 2013

Seepersad, G. (2012) Reduction of initial convergence period in GPS-PPP data processing, [*Msc Thesis*] York University, Toronto, Canada.

Seepersad, G. and S. Bisnath (2012). "Reduction of Precise Point Positioning convergence period." Proceedings of ION GNSS 2012, Nashville, Tennessee, pp. 3742-3752.

SOPAC (2013) Site Information Tool, http://sopac.ucsd.edu/cgi-bin/SITe.cgi, accessed March 2013.

Zumberge, J.F., M.B. Heflin, D.C. Jefferson, and M.M. Watkins (1997) Precise point positioning for the efficient and robust analysis of GPS data from large networks.", *Journal of Geophysical Research*, Vol. 102, No. B3, pp. 5005-5018.